Available online at www.sciencedirect.com
ScienceDirect
Microporous and Mesoporous Materials 103 (2007) 40–47
MICROPOROUS AND MESOPOROUS MATERIALS
www.elsevier.com/locate/micromeso

# A contribution to the physicochemical characterization of nonstoichiometric salts of tungstosilicic acid

Luis R. Pizzio, Mirta N. Blanco *

*Centro de Investigación y Desarrollo en Ciencias Aplicadas "Dr. J. J. Ronco" (CINDECA), Departamento de Química, Facultad de Ciencias Exactas, UNLP-CONICET, Calle 47 N[o] 257, 1900-La Plata, Argentina*

Received 6 November 2006; received in revised form 15 January 2007; accepted 21 January 2007
Available online 26 January 2007

**Abstract**

Nonstoichiometric cesium and rubidium salts of tungstosilicic acid (TSA) were synthesized by precipitation. These solids are insoluble in water, due to the low solvation energy of large cations, have high specific surface area, and a mainly microporous structure. In turn, nonstoichiometric potassium salts prepared by solution evaporation have a low specific surface area and porosity, high solubility in water, and a negligible porosity. All the synthesized tungstosilicates presented a cubic structure, with a lattice parameter that slightly decreases in the order $Cs^+ > Rb^+ \cong K^+$ salts.

The salts displayed the characteristic FT-IR bands of TSA, though the band assigned to the stretching of the W=O terminal bond presented a slight widening and a shoulder, and the band attributed to a bridged W—O—W bond was shifted to a lower wavenumber and showed a shoulder. Such effects are indicative of the interaction between the $[SiW_{12}O_{40}]^{4-}$ anion and the alkaline cations.

Assuming that an increase in $^1H$ MAS-NMR chemical shift is due to a higher acid strength, the cesium salts would have acid sites with higher acid strength than the others. The potassium salts, however, presented protons in different acid environments, with a low proportion of very strong acid sites.

The acidity measurement by potentiometric titration with *n*-butylamine also showed that the cesium salts have acid sites with higher strength than those of rubidium. The same behavior was observed for the potassium salts, which exhibited an acid strength higher than expected. The number of protons determined by titration decreased in the order $Cs^+ > Rb^+ \cong K^+$ salts and also decreased for the more substituted salts.


*Keywords:* Tungstosilicic acid; Salts; Synthesis; Characterization; Microporous materials

## 1. Introduction

The use of solids containing a pore network is important for heterogeneous catalysis because their higher surface area leads to higher activity in surface reactions. In addition, the presence of pores of adequate size allows a better transport of reactants or products to or from the active sites. We have recently informed that the conversion in alcohol dehydration, carried out using Keggin heteropolyacids (HPA) supported on carbon with different textural properties, depends on the alcohol molecular size compared to the mean pore diameter of the catalysts, whereas the selectivity to alkenes is also related to cyclodimer molecular size formed by certain alkenes in acidic medium [1].

The low catalytic yield, displayed by bulk tungstophosphoric and tungstosilicic acids in some acid reactions, is due to their low specific surface area. This can be considerably increased by supporting the HPA on adequate porous solids [2] or by using insoluble salts of HPA. Some salts of Keggin-type heteropolyacids showed high surface areas

* Corresponding author. Tel.: +54 0221 4211353.
*E-mail address:* mnblanco@quimica.unlp.edu.ar (M.N. Blanco).

1387-1811/$ - see front matter © 2007 Elsevier Inc. All rights reserved.
doi:10.1016/j.micromeso.2007.01.036

and microporous structure. These properties depend upon the metal atoms of the heteropolyanion primary structure and the nature of the countercation [3]. Thus, the stoichiometric ammonium salt of tungstophosphoric acid, unlike its parent acid, presented a high surface area, microporous structure, and a high activity and selectivity in the conversion of methanol into hydrocarbons [4].

The synthesis of nonstoichiometric $K^+$ or $Cs^+$ salts of $H_3PW_{12}O_{40}$, with a replacement between two and three protons, leads to porous solids with high specific surface area compared to the bulk heteropolyacid [5]. Due to their high surface proton density, insoluble salts have given excellent catalytic activity in diverse acid reactions, such as the isomerization of *n*-butene [6]. The salt microporosity was attributed to a rotation and translation of the anions that allow the terminal oxygens to be distant from each other, caused by the substitution of the protons by large cations. As a consequence, the interstitial voids can be connected forming channels, resulting in a porous network that is dependent on the cation size. On the other hand, the presence of residual protons in the salts also influences the pore structure [3].

The salt stoichiometry, the nature and source of the cations, and the thermal treatment are some of the variables that influence their properties. Salts with a low cation amount may contain large quantities of protons and exhibit small surface area. Lapham and Moffat [3] have reported that the residual protons may block the pores and reduce the accessible surface area. In turn, the thermal treatment of ammonium salts of tungstophosphoric acid, prepared with excess of ammonium carbonate with respect to the stoichiometric amount, leads to high surface area due to evolution of carbon dioxide.

The salts of the tungstophosphoric acid are the most stable and the most extensively studied, whereas those corresponding to the tungstosilicic acid have received less attention. Nevertheless, there are some reports dealing with their characterization or their use as acidic catalysts. For example, Huang et al. [7] have reported that salts of tungstosilicic acid, in which only one proton is replaced, such as $LiH_3SiW_{12}O_{40}$ or $Mg_{0.5}H_3SiW_{12}O_{40}$, show high activity in the condensation of formaldehyde and methyl formate. Since most of the neutral salts had no activity, they assumed that free protons in the salts are responsible for their activity.

Recently, we have studied the characteristics of nonstoichiometric cesium and potassium salts of tungstophosphoric acid, and also the bulk acid impregnated on them, as well as their behavior in the esterification of acetic acid and isoamyl alcohol [5]. We found a straight correlation between the catalytic activity and the acidic properties of the studied solids. We also found that the acid strength is a decisive factor in the catalytic behavior of cesium or rubidium tungstosilicate, but that the textural properties of them must also be taken into account [8]. In order to gain deeper insight into the alkaline tungstosilicates, the aim of this work is to make a contribution to the study of the characteristics of nonstoichiometric $Cs^+$, $Rb^+$, or $K^+$ salts of tungstosilicic acid, $Cs(Rb)(K)_{4-x}H_xSiW_{12}O_{40}$. The physicochemical characterization, the thermal behavior, and the acidic properties determined by means of $^1H$ NMR and potentiometric titration with *n*-butylamine are reported. The results are discussed and compared in relation to the properties of the countercation, bearing in mind that the salts can be used in acidic reactions.

## 2. Experimental

### 2.1. Salt synthesis

Tungstosilicic acid (Fluka p.a.), cesium chloride (Merck p.a.), rubidium nitrate (Alfa Aesar p.a.), and potassium chloride (Merck p.a.) were used without further purification. Nonstoichiometric cesium and rubidium salts, $Cs_{3.4}H_{0.6}SiW_{12}O_{40}$, $Cs_{3.8}H_{0.2}SiW_{12}O_{40}$, $Rb_{2.9}H_{1.1}SiW_{12}O_{40}$, $Rb_{3.8}H_{0.2}SiW_{12}O_{40}$ were synthesized by slowly adding, with continuous stirring, 11.5 or 12.5 ml of a CsCl 3 M solution and 14.5 or 19 ml of a $RbNO_3$ 2 M solution to 100 ml of a 0.1 M solution of $H_4SiW_{12}O_{40}$ in water. The precipitate was separated by centrifugation, then washed with distilled water, and dried at 70 °C for 24 h. Nonstoichiometric potassium salts, $K_{3.3}H_{0.7}SiW_{12}O_{40}$ and $K_{3.8}H_{0.2}SiW_{12}O_{40}$, were obtained by evaporation of a solution containing 11 or 12.5 ml of a KCl 3 M solution and the same TSA solution used for obtaining the other salts. They were similarly thermally treated.

### 2.2. Salt characterization

#### 2.2.1. Textural properties

The salts were studied by nitrogen adsorption/desorption at −196 °C, using Micromeritics Acccusorb 2100E equipment. Samples were previously treated by outgassing at 100 °C for 1 h. The specific surface area ($S_{BET}$) was calculated using the Brunauer–Emmett–Teller equation applied to the adsorption branch of the adsorption isotherm. The equivalent microporous surface ($S_{micro}$) and the microporous volume ($V_{micro}$) were calculated using the *t*-plot method [9], and the statistical thickness *t* was deduced from Lecloux standard isotherm [10].

#### 2.2.2. X-ray diffraction

The X-ray diffraction (XRD) patterns of the solids were recorded with Philips PW-1732 equipment with a built-in recorder, using Cu $K_\alpha$ radiation, nickel filter, 30 mA and 40 kV in the high voltage source, and scanning angle between 5 and 60° $2\theta$ at a scanning rate of 1° per minute.

#### 2.2.3. Fourier transform infrared spectroscopy

The Fourier transform infrared (FT-IR) spectra of the salts were recorded with Bruker IFS 66 FT-IR equipment. Pellets of ca. 1% w/w of the sample in KBr were prepared in a self-made device. A measuring range of 400–1500 $cm^{-1}$ was studied, the resolution being 2 $cm^{-1}$.

*2.2.4. Thermogravimetric and differential thermal analysis*

The salts were studied by thermogravimetric (TGA) and differential thermal analysis (DTA) using a Shimadzu DT 50 thermal analyzer. The experiments were performed up to 700 °C at a heating rate of 10 °C/min under helium flow (20 $cm^3$/min), using 20–25 mg of sample, respectively. Platinum cells were used as sample holders with $\alpha$-$Al_2O_3$ as reference.

*2.2.5. $^1H$ nuclear magnetic resonance*

The $^1H$ nuclear magnetic resonance ($^1H$ MAS NMR) spectra were obtained with Bruker Avance ASX-400 equipment with a sample holder of 2.5 mm diameter and 10 mm in height, using 2.7 μs pulses, a repetition time of 5 s, and a frequency of 400.13 MHz, the resolution being 0.953 Hz per point and the spin rate 20 kHz. Tetramethylsilane was employed as external reference.

*2.2.6. Potentiometric titration with n-butylamine*

Potentiometric titration was used to evaluate the acidic characteristics of the solids. To this end, 50 mg of solid suspended in 45 ml acetonitrile was stirred for 3 h. Then, the titration was carried out with a solution of *n*-butylamine in acetonitrile (0.05 N) at a flow rate of 0.05 $cm^3$/min. The electrode potential variation was measured in an Instrumentalia S.R.L. digital pH meter with a double-junction electrode.

## 3. Results

The nonstoichiometric cesium and rubidium salts of tungstosilicic acid (TSA) are insoluble in water. Their insolubility can be attributed to the low solvation energy of large cations, the enthalpies of hydration being −296 and −263 kJ/mol for $Rb^+$ and $Cs^+$ ions, respectively [11].

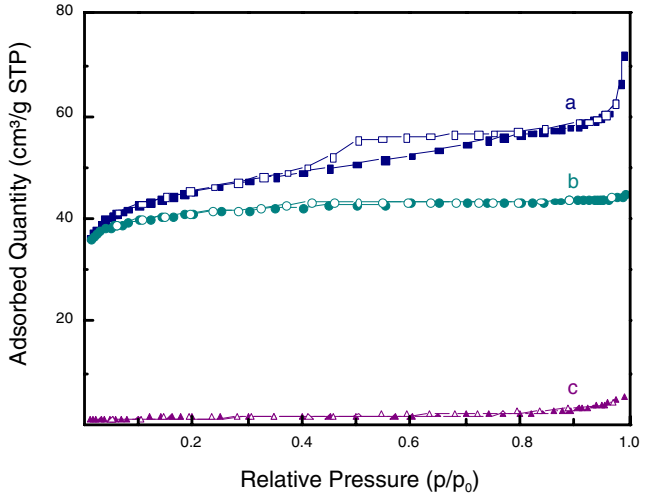


Fig. 1. Nitrogen adsorption/desorption isotherms at −196 °C of (a) $Cs_{3.8}H_{0.2}SiW_{12}O_{40}$, (b) $Rb_{3.8}H_{0.2}SiW_{12}O_{40}$, (c) $K_{3.8}H_{0.2}SiW_{12}O_{40}$ salts. Adsorption branch (full symbols), desorption branch (open symbols).

The nitrogen adsorption/desorption isotherms at −196 °C are shown in Fig. 1 for the more substituted salts, being similar for the others. A sharp initial increase of the adsorbed volume at low relative pressure, characteristic of microporous solids, can be observed for both the cesium and rubidium salts, while a hysteresis is observed for the cesium tungstosilicates, indicative of the presence of some mesopores. For the potassium salts, the adsorbed volume is very low. The high specific surface area ($S_{BET}$) of the cesium and rubidium salts (Table 1) is a consequence of the small size of the primary particles. In all cases the surface area was considerably higher than that of the tungstosilicic acid, which is 2 $m^2$/g, and this is mainly due to the presence of micropores. According to the calculated $S_{micro}$ values (Table 1), approx. 80% of the total surface area came from the microporous structure for the rubidium salts, and approximately 65% for those of cesium. The micro- and mesopores present in this type of salt are the result of the formation of interparticle voids by agglomeration of the primary particles [6]. In turn, dissimilar behavior was observed for the nonstoichiometric potassium salts, which have a specific surface area (Table 1) close to that of TSA, and are soluble in water. The enthalpy of hydration is −325 kJ/mol for $K^+$ cation [11]. The potassium tungstosilicates must be synthesized in a different way than the previous salts, by evaporation of the solution, because they do not precipitate as the others do. The pore distribution obtained from plots of $dV/dr$ as a function of $r$ (pore radius) is shifted toward higher $r$ for the potassium salts when compared with those of cesium and rubidium. While the latter mainly presented pores with a mean diameter lower than 2 nm, and a low proportion with 2.7 nm, the potassium salts mainly showed pores with diameters larger than 3.3 nm. The negligible porosity in the latter samples may be attributed to the different synthesis method that led to larger sized microcrystals. Similar results have been already reported by Moffat [12] who pointed out that the stoichiometric potassium salt of tungstosilicic acid has little or no microporosity.

The XRD patterns of the nonstoichiometric synthesized salts (Fig. 2) were almost alike, though the potassium tungstosilicates were less well crystallized. They showed lines similar to those corresponding to the cubic phase of the $Cs_4SiW_{12}O_{40}$ salt (JCPDS 46-0221). The lines corresponding to the parent acid $H_4SiW_{12}O_{40} \cdot 22H_2O$ were not present, nevertheless the patterns exhibited lines similar to those of $H_4SiW_{12}O_{40} \cdot 6H_2O$, though slightly shifted. The behavior of the alkaline tungstosilicate resembles what has been reported in the literature about the cubic phase of the $Cs_3PW_{12}O_{40}$ salt [13].

It has been already reported that the neutral cesium and rubidium salts of $H_4SiW_{12}O_{40}$ crystallize in cubic structure and that the di- and tri-substituted salts present the same crystalline structure [14]. The lattice parameter ($a$) was calculated using the lines corresponding to the [1 1 0], [2 2 2], and [4 0 0] planes (lines near 10.5, 26, and 30° 2$\theta$, respectively). The $a$ value was nearly the same for both salts of

Table 1
Characteristics of the cesium, rubidium and potassium tungstosilicates

| Sample | $S_{BET}$ ($m^2/g$) | $S_{micro}$ ($m^2/g$) | $V$ ($cm^3/g$) | $V_{micro}$ ($cm^3/g$) | $a$ (nm) | $I_{110}/I_{222}$ | $\delta$ (ppm) |
|---|---|---|---|---|---|---|---|
| $Cs_{3.4}H_{0.6}SiW_{12}O_{40}$ | 162 | 100 | 0.11 | 0.04 | 1.180 | 0.189 | 5.2 |
| $Cs_{3.8}H_{0.2}SiW_{12}O_{40}$ | 169 | 106 | 0.18 | 0.07 | 1.178 | 0.176 | 4.5 |
| $Rb_{2.9}H_{1.1}SiW_{12}O_{40}$ | 130 | 104 | 0.07 | 0.03 | 1.164 | 0.410 | 4.3 |
| $Rb_{3.8}H_{0.2}SiW_{12}O_{40}$ | 137 | 110 | 0.07 | 0.03 | 1.162 | 0.277 | 4.3 |
| $K_{3.3}H_{0.7}SiW_{12}O_{40}$ | 5 | | | | 1.161 | 0.466 | 4.3; 5.6; 10 (w) |
| $K_{3.8}H_{0.2}SiW_{12}O_{40}$ | 5 | | | | 1.155 | 0.391 | 4.0; 5.6 (m); 10 (v w) |

$S_{BET}$: specific surface area, $S_{micro}$: specific microporous surface area, $V$: maximum pore volume, $V_{micro}$: microporous volume, $a$: lattice parameter, $I_{110}/I_{222}$: ratio of the intensity of the lines corresponding to [1 1 0] and [2 2 2] planes, $\delta$: $^1H$ MAS-NMR chemical shift (m, w and v w indicate medium, weak and very weak peaks).

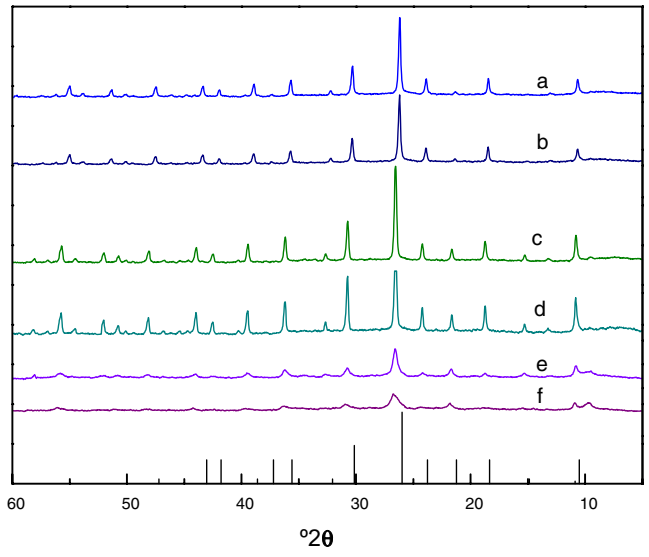


Fig. 2. XRD patterns of: (a) $Cs_{3.4}H_{0.6}SiW_{12}O_{40}$, (b) $Cs_{3.8}H_{0.2}SiW_{12}O_{40}$, (c) $Rb_{2.9}H_{1.1}SiW_{12}O_{40}$, (d) $Rb_{3.8}H_{0.2}SiW_{12}O_{40}$, (e) $K_{3.3}H_{0.7}SiW_{12}O_{40}$, (f) $K_{3.8}H_{0.2}SiW_{12}O_{40}$ salts, and $Cs_4SiW_{12}O_{40}$ salt (JCPDS 46-0221) as bars.

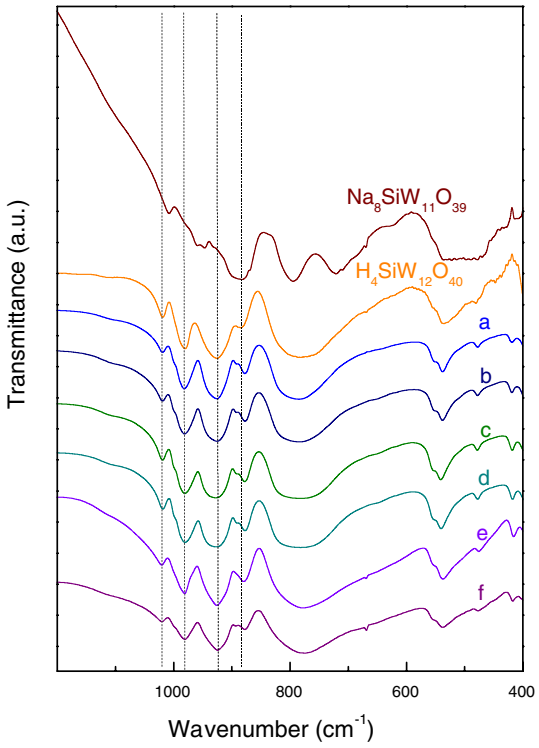


Fig. 3. FT-IR spectra of: (a) $Cs_{3.4}H_{0.6}SiW_{12}O_{40}$, (b) $Cs_{3.8}H_{0.2}SiW_{12}O_{40}$, (c) $Rb_{2.9}H_{1.1}SiW_{12}O_{40}$, (d) $Rb_{3.8}H_{0.2}SiW_{12}O_{40}$, (e) $K_{3.3}H_{0.7}SiW_{12}O_{40}$, and (f) $K_{3.8}H_{0.2}SiW_{12}O_{40}$ salts, TSA, and $Na_8SiW_{11}O_{40}$.

the same cation and only slightly decreased in the order $Cs^+ > Rb^+ \cong K^+$ salts (Table 1). In addition, the ratio of the intensity of the line corresponding to the [1 1 0] plane and that of the [2 2 2] plane was calculated (Table 1). It can be seen that these values increased in the order $Cs^+ < Rb^+ < K^+$ salts, and decreased as the replacement by alkaline cation increased, though the variation was very slight for the cesium tunstosilicates. This may be considered as indicative of a decrease in microporosity of the salts [15] in the same above-mentioned order, in agreement with the results from analysis of the data obtained by nitrogen adsorption/desorption at −196 °C.

On the other hand, the FT-IR spectrum of bulk TSA at room temperature displayed bands at 1020, 982, 926, 884, 778, and 541 $cm^{-1}$. Such bands agreed well with those referred to in the literature for TSA [16]. The same characteristic bands were found to be present in all the synthesized salts (Fig. 3). The band at 982 $cm^{-1}$, assigned to the stretching of the W=O terminal bond, presented a slight widening and a shoulder at 999 $cm^{-1}$. Besides, the band at 884 $cm^{-1}$, attributed to a bridged W—O—W bond, formed by oxygens that link the four $W_3O_{13}$ triads that form the peripheral structure of the anion, was shifted to a lower wavenumber and showed a shoulder at 892 $cm^{-1}$. These effects may appear as a result of the interaction between the $[SiW_{12}O_{40}]^{4-}$ anion and the alkaline cations. A transformation of the $[SiW_{12}O_{40}]^{4-}$ species into the $[SiW_{11}O_{39}]^{8-}$ lacunar phase during the salt synthesis was not detected by this technique. The main bands of the latter are placed at 1008, 959, 946, 882, 869, 794 and 720 $cm^{-1}$ (Fig. 3).

The DTA diagram of $H_4SiW_{12}O_{40} \cdot 22\,H_2O$ displayed two endothermic peaks with maxima at 68 and 187 °C, assigned to water loss, and an exothermic peak with maxima at 534 °C due to the structure decomposition of the Keggin anion. On the other hand, the diagram obtained by TGA presented two weight losses clearly distinguishable

below 250 °C [8]. The first one is assigned to the evolution of physisorbed water that leads to the formation of the hexahydrate $H_4SiW_{12}O_{40} \cdot 6H_2O$, whereas the second step is due to the loss of crystallization water producing the anhydrous species $H_4SiW_{12}O_{40}$. The weight loss that appears for TSA between 250 and 500 °C is due to evolution of two molecules of constitutional water by each $H_4SiW_{12}O_{40}$, as a result of the complete deprotonation of the heteropolyacid, as has been reported for the $H_3PW_{12}O_{40}$ acid [17].

The alkaline metal salts presented two unresolved endothermic peaks below 150 °C in the DTA diagrams (not shown), corresponding to the loss of physisorbed water. The thermal stability of the Keggin structure of $[SiW_{12}O_{40}]^{4-}$ anion is higher for the salts compared to the acid, those of cesium and rubidium being thermally more stable than those of potassium. For the cesium salts, an exothermal peak assigned to the anion decomposition appeared at 670 and 680 °C, whereas the beginning of this peak seems to appear in the diagrams corresponding to the rubidium samples near 700 °C, the maximum attainable temperature. In turn, the potassium salts presented a wide decomposition band from 580 °C on, with a maximum at 650 °C.

The $^1$H MAS-NMR spectra of the cesium and rubidium salts showed a single resonance, broader than that of TSA (Fig. 4), which displayed a unique sharp peak at a chemical shift $\delta = 6.9$ ppm. As summarized in Table 1, the main resonance observed in the salt spectra was shifted upfield relative to that of TSA. While both rubidium samples displayed $\delta = 4.3$ ppm, the $Cs_{3.8}H_{0.2}SiW_{12}O_{40}$ salt presented a peak at similar position (4.5 ppm), and the less substituted cesium sample at $\delta = 5.2$ ppm. In turn, the potassium salts showed two overlapped peaks with maxima approximately at 4–4.3 and 5.6 ppm, and a weak peak approximately at 10 ppm. The results are indicative of different proton environments according to the cation and the substitution degree. For the cesium salts, the proton resonance moved upfield for the more substituted sample, in a similar way as has been reported by Parent and Moffat [18] for silver, thallium and cesium salts of tungstophosphoric acid. The residual protons in the non stoichiometric potassium salts showed the more intense signal in a position similar to that of rubidium samples and the other, with lower intensity, was placed near that of $Cs_{3.4}H_{0.6}SiW_{12}O_{40}$ salt.

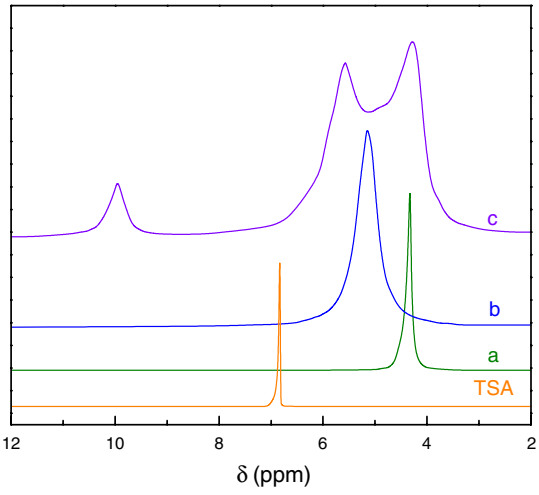


Fig. 4. $^1$H NMR spectra of: (a) $Rb_{2.9}H_{1.1}SiW_{12}O_{40}$, (b) $Cs_{3.4}H_{0.6}SiW_{12}O_{40}$ and (c) $K_{3.3}H_{0.7}SiW_{12}O_{40}$ salts, together with TSA spectra.

It has been reported that the chemical shift in zeolites correlates with proton acidity [19]. Though for heteropolycompounds the relationship between acid strength and proton chemical shift is not straightforward due to proton mobility [20], the technique can still be used when the samples correspond to the same Keggin stable anion [21]. The cesium salts would have acid sites with higher acid strength than those of rubidium, taking into account that an increase in chemical shift is considered to be indicative of a higher acid strength [22] due to more acidic protons are less shielded because they have less electrons in its vicinity [21]. The potassium salts, however, showed protons in different acid environments, with a low proportion of very strong acid sites.

By means of potentiometric titration with *n*-butylamine, it is possible to estimate the strength and the number of acid sites present in the salts. It is considered that the initial electrode potential ($E_i$) indicates the maximum strength of the acid sites, and the value from which the plateau (meq amine/mmol salt) is reached is indicative of the total number of acid sites that the titrated solid presents. Otherwise, the end point of the titration, given by the inflexion point of the curve, is a good measure to carry out a comparison of the acidity of different samples.

The strength of the acid sites can be classified according the following scale: $E_i > 100$ mV (very strong sites); $0 < E_i < 100$ mV (strong sites); $-100 < E_i < 0$ mV (weak sites), and $E_i < -100$ mV (very weak sites) [23].

The potentiometric titration curves of the partially substituted tungstosilicates are shown in Fig. 5a–c, for the cesium, rubidium, and potassium salts, respectively. It is observed that the cesium samples present very strong acid sites ($E_i = 450$ mV), and the number of titrated protons determined by the inflexion point of the titration curves varied in the following order: $Cs_{3.4}H_{0.6}SiW_{12}O_{40} > Cs_{3.8}H_{0.2}SiW_{12}O_{40}$. These salts have higher acid strength than those of rubidium ($E_i = 80$ mV), whereas the number of titrated protons for the latter followed the same trend, that is $Rb_{2.9}H_{1.1}SiW_{12}O_{40} > Rb_{3.8}H_{0.2}SiW_{12}O_{40}$. The potassium salts exhibited an acid strength higher than expected ($E_i = 310$–$350$ mV) and the number of titrated protons in an order similar to the others, that is $K_{3.3}H_{0.7}SiW_{12}O_{40} > K_{3.8}H_{0.2}SiW_{12}O_{40}$. This may be a result of residual protons from the parent heteropolyacid owing to the different synthesis method used. In turn, the acid strength of all the salts was lower than that determined for bulk $H_4SiW_{12}O_{40}$ ($E_i = 740$ mV).

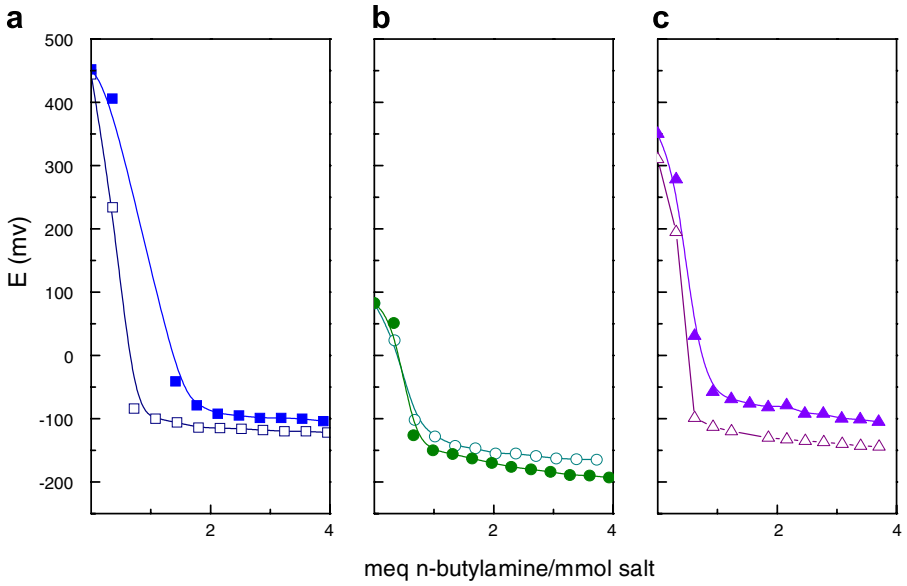


Fig. 5. Curves obtained by potentiometric titration with *n*-butylamine of the salts: (a) $Cs_{3.4}H_{0.6}SiW_{12}O_{40}$ (■), $Cs_{3.8}H_{0.2}SiW_{12}O_{40}$ (□), (b) $Rb_{2.9}H_{1.1}SiW_{12}O_{40}$ (●), $Rb_{3.8}H_{0.2}SiW_{12}O_{40}$ (○), and (c) $K_{3.3}H_{0.7}SiW_{12}O_{40}$ (▲), $K_{3.8}H_{0.2}SiW_{12}O_{40}$ (△).

## 4. Discussion

The cation nature may have a great influence on the final properties of the salts of HPA. The salts with small cations such as $Na^+$ (named A type salts) are highly soluble in water or other polar solvents and have a low specific surface area, while the salts of large cations such as $Cs^+$ (named B type salts) are insoluble in water and possess a high specific surface area.

The salts of alkaline cations of tungstosilicic acid have been less studied than those of tungstophosphoric acid, possibly due to the lower acidic nature of the former [24]. There are some studies related to the textural properties of such salts, e.g. [25], and others about the characterization by means of FT-IR and XRD have also been reported [14,26]. Their catalytic behavior was tested in some reactions. Among them, He et al. [27] have presented results about the coupling of formaldehyde and methyl formate using different salts of TSA as catalysts. Izumi et al. [28] have found that $Cs_2H_2SiW_{12}O_{40}$ is more active than $Rb_2H_2SiW_{12}O_{40}$ in the benzene benzylation, though $K_2H_2SiW_{12}O_{40}$ exhibited an intermediate conversion. Besides, the beneficial use of potassium salts of tungstosilicic acid for esterification reactions was claimed in a patent [29].

Here we performed a systematic study of the characterization of $Cs^+$, $Rb^+$, and $K^+$ salts of TSA by different physicochemical techniques in order to use them in acidic reactions.

It may be remarked that, unlike $K^+$ and $Cs^+$ salts of tungstophosphoric acid [5], $K^+$ and $Cs^+$ salts of TSA behave alike with regard to their solubility. Cesium salts, and also rubidium ones, are insoluble in water [14], while potassium salts are soluble. The different solubility in water has been reported by Taylor et al. [30] and may be inferred from the textural data informed. In these papers, the surface area of stoichiometric potassium tungstosilicate is around 3 $m^2/g$, resembling that of TSA. Similar values were measured in our nonstoichiometric potassium samples (5 $m^2/g$) while the other salts exhibited a specific surface area around 130–160 $m^2/g$, those synthesized with cesium as countercation being higher (Table 1). The properties and size of the cations give an ion pattern that leads to the formation of channels and to mainly microporous materials, with higher pore volume for the cesium salts. The microporous structure was found to depend on the size of the alkaline cation, as well as on the extent of substitution degree and the preparation conditions, as has been already reported for tungstophosphates [31].

The secondary structure was affected by the cation nature. All the salts presented a body-centered cubic structure. Nevertheless, the unit cell of the cesium salts is larger, as reflected by the shifting of the lines in the diffractograms to lower °2$\theta$ angles (Fig. 2). The calculated lattice parameters are in accordance with Vakulenko et al. [14], who have reported values of 1.1791 and 1.1613 nm for the stoichiometric cesium and rubidium salts, respectively. For the same tungstosilicates there is also an agreement with Taylor et al. [30], but the value for the potassium salt is different. They have reported 1.276 nm for the stoichiometric salt, while the potassium tungstosilicates synthesized here followed the trend expected according to the cation size, presenting a somewhat lower lattice parameter than the other salts studied. On the other hand, the lattice parameters of all the samples are slightly lower than that estimated for TSA (1.204 nm). Clearly, the hydrated proton leads to higher separation of the crystallographic planes.

However, at first sight the changes in the primary structure of the heteropolysalts seem less marked. As expected,

the nonstoichiometric salts of tungstosilicic acid synthesized in this work retained the Keggin structure of the heteropolyacid. Nevertheless, the effect of the presence of the alkaline cation was observed through certain features that appeared in the FT-IR spectra when compared to the TSA spectrum. Both the shoulder at 999 $cm^{-1}$ overlapped to the band assigned to W=O bond and that at 892 $cm^{-1}$ on the band assigned to a bridged W—O—W bond, in addition to the shift toward a lower wavenumber, may be assumed to be caused by the presence of the cations. So, it is seen that not only terminal oxygen is affected, but also bridged oxygen.

Though the position of the main bands was slightly affected, the above-mentioned effects were more evident than those caused by $Cs^+$ or $K^+$ in the salts of tungstophosphoric acid [5]. It may be assumed that the structure is slightly less rigid when the central atom is Si, due to its lower charge, and hence more likely to be affected by anion–anion and anion–cation interactions. In particular, although the asymmetric stretching that leads to the band at 884 $cm^{-1}$ is not a pure vibration and can have some bending character, the observed shifting could be due to perturbations caused by anion–cation interactions, which lead to a decrease in the band frequency [26].

The other interesting result is related to the higher stability of the salts compared to the parent acid, which is similar to the behavior of nonstoichiometric salts of tungstophosphoric acid [5]. It has been reported that the thermal stability of $M_{4-x}H_xSiW_{12}O_{40} \cdot nH_2O$ samples depends on the neutralization degree as well as on the cation nature [14]. The decomposition is noted by the appearance of exothermal peaks in the corresponding DTA diagrams in the temperature range 500–750 °C. For the salts synthesized here, the decomposition peak near 700 °C when cesium is the countercation and the beginning of the peak for rubidium countercation were clearly observed, while the potassium salt began to decompose at a lower temperature.

For their use as heterogeneous catalysts in acidic reactions, knowledge of the acidic properties is important. The observed behavior is correlated with the other results about the effect of the cation size on the properties of the salts. Both techniques used revealed that the acid strength and the number of titrated protons are higher in the nonstoichiometric cesium salts than in the rubidium samples. In turn, the potassium salt presented an acid strength higher than expected, though the number of titrated protons is low. The results on acid strength would explain the behavior reported in the literature about $K_2H_2SiW_{12}O_{40}$ used as catalyst in benzene benzylation, which exhibited an intermediate conversion between those corresponding to cesium and rubidium salts with the same stoichiometry [28].

The acid strength of the heteropolyacids is related to the proton mobility, which partly depends on the distribution of the negative charge on the oxygens of the heteropolyanion. An increase of the charge on these atoms causes an increase of the coulombic type interaction with the protons and, therefore, a decrease of their mobility, which leads to a decrease in the acid strength. The partial substitution by alkaline cations alters the mobility of the remaining protons, possibly as a result of a change in charge distribution over the oxygen atoms. The broadening of the $^1H$ NMR peaks with respect to that of bulk TSA may be due to protons more localized on the bridging W—O—W oxygens, as was reported for tungstophosphoric acid supported on $TiO_2$ [32]. This fact would be in agreement with the lower acid strength determined by potentiometric titration and the lower chemical shift values of the salts when compared with those of bulk TSA.

He et al. [33] have verified that the activity of the $M_1H_2PW_{12}O_{40}$ salts in the condensation of formaldehyde and methyl formate depends on the nature of the alkaline metal M, and that it decreases in the order K > Na > Li, the same order of the decrease in ionic radius. These results, among others, encourage us to state that the alkaline tungstosilicates are good candidates to be used in acidic reactions. Their behavior in the tetrahydropyranylation–depyranylation of phenol was studied [8], and we found that the nonstoichiometric cesium salts show very high catalytic activity in the phenol tetrahydropyranylation reaction and in the tetrahydropyranyl ether deprotection, while the rubidium salts are only active in the depyranylation reaction. In both reactions, the desired product was obtained selectively, without side product formation. The acid strength was a key factor in the catalytic behavior of the salts, and their textural properties must also be taken into account. So, the present study may help in the selection of the salt, according to the reaction in which it will be used as catalyst, taking into account their acid strength requirements and also the type of substituents in the compounds involved in the chemical transformation.

## 5. Conclusions

By partial neutralization of aqueous solutions of tungstosilicic acid with solutions containing cesium or rubidium cations, mainly microporous solids were obtained, which are insoluble in water, and thermally more stable and with higher surface area than bulk TSA. In turn, using solutions with potassium cations, evaporation of the solution was needed due to these salts are soluble in water. They have a specific surface area close to that of TSA, and show low porosity, which may be a result of the different preparation method. All the salts exhibited a cubic structure, with a lattice parameter that slightly decreases in the same order as the cation radius does.

While during the synthesis of the salts the Keggin structure remains unaltered, an interaction between the tungstosilicate anion and the alkaline cations was found. It was clearly evidenced that not only terminal oxygens of the primary structure are affected, but also bridged oxygens.

It can be also stated that the cation nature and the neutralization degree of the salts allow the acid strength and the total number of acid sites to be varied. The cesium salts

have acid sites with higher acid strength than those of rubidium or potassium, though the potassium tungstosilicates have protons in different acidic environments, with a low proportion of very strong acid sites. So, the synthesized salts may be used, according to their characteristics, as replacement of classical homogeneous catalysts in different acidic reactions.

## Acknowledgments

The authors thank A. Sangiácomo, E. Soto, N. Bernava and G. Valle for their experimental help, B. Revel and A. Rives for NMR measurements, and Antorchas Foundation, CONICET and UNLP for their financial support.

## References

[1] L. Pizzio, P. Vázquez, C. Cáceres, M. Blanco, E. Alesso, M.I. Erlich, R. Torviso, L. Finkielsztein, B. Lantaño, G. Moltrasio, J. Aguirre, Catal. Lett. 93 (2004) 67.
[2] L.R. Pizzio, C.V. Cáceres, M.N. Blanco, Appl. Catal. 167 (1998) 283.
[3] D. Lapham, J.B. Moffat, Langmuir 7 (1991) 2273.
[4] H. Hayashi, J.B. Moffat, J. Catal. 83 (1983) 192.
[5] L.R. Pizzio, M.N. Blanco, Appl. Catal. A: General 255 (2003) 265.
[6] T. Okuhara, N. Mizuno, M. Misono, Adv. Catal. 41 (1996) 221.
[7] W. Huang, D. He, J. Liu, Q. Zhu, Appl. Catal. 199 (2000) 93.
[8] G.P. Romanelli, J.C. Autino, M.N. Blanco, L.R. Pizzio, Appl. Catal. A: General 295 (2005) 209.
[9] R.Sh. Mikhail, S. Brunauer, E.E. Bodor, J. Colloid Interface Sci. 26 (1968) 45.
[10] A. Lecloux, J.P. Pirard, J. Colloid Interface Sci. 70 (1979) 265.
[11] P.D. Metelski, T.W. Swaddle, Inorg. Chem. 38 (1999) 301.
[12] J.B. Moffat, Polyhedron 5 (1986) 261.
[13] G.M. Brown, M.R. Noe-Spirlet, W.R. Busing, H.A. Levy, Acta Cryst. B 33 (1977) 1038.
[14] A. Vakulenko, Y. Dobrovolsky, L. Leonova, A. Karelin, A. Kolesnikova, N. Bukun, Solid State Ion. 136 (7) (2000) 285.
[15] J.B. McMonagle, J.B. Moffat, J. Colloid Int. Sci. 101 (1984) 479.
[16] C. Rocchiccioli-Deltcheff, R. Thouvenot, R. Franck, Spectrochim. Acta 32 A (1976) 587.
[17] N. Essayem, G. Coudurier, M. Fournier, J. Védrine, Catal. Lett. 34 (1995) 223.
[18] M.A. Parent, J.B. Moffat, Catal. Lett. 48 (1997) 135.
[19] V.M. Mastikhin, S.M. Kulikov, A.V. Nosov, I.V. Khozevnikov, I.L. Mudrakovsky, M.N. Timofeeva, J. Mol. Catal. 60 (1990) 65.
[20] P.M. Rao, A. Wolfson, S. Kababya, S. Vega, M.V. Landau, J. Catal. 232 (2005) 210.
[21] N. Essayem, Y.Y. Tong, H. Jobic, J.C. Vedrine, Appl. Catal. A: General 194 (5) (2000) 109.
[22] M.A. Gao, J.B. Moffat, Catal. Lett. 42 (1996) 135.
[23] R. Cid, G. Pecci, Appl. Catal. 14 (1985) 15.
[24] I.V. Khozhevnikov, Chem. Rev. 98 (1998) 171.
[25] D.B. Taylor, J.B. McMonagle, J.B. Moffat, J. Colloid Int. Sci. 108 (1985) 278.
[26] C. Rocchiccioli-Deltcheff, M. Fournier, R. Franck, R. Thouvenot, Inorg. Chem. 22 (1983) 207.
[27] D. He, W. Huang, J. Liu, Q. Zhu, J. Molec. Catal. A: Chem. 145 (1999) 335.
[28] Y. Izumi, M. Ogawa, W. Nohora, K. Urabe, Chem. Lett. (1992) 1987.
[29] A. Fu, E. Kadowaki, T. Higashi, H. Uchida, US Patent Application 20030135069, 2003.
[30] D.B. Taylor, J.B. McMonagle, J.B. Moffat, J Colloid Int. Sci. 108 (1985) 278.
[31] A. Corma, A. Martínez, C. Martínez, J. Catal. 164 (1996) 422.
[32] J.C. Edwards, C.Y. Thiel, B. Benac, J.F. Knifton, Catal. Lett. 51 (1998) 77.
[33] D. He, W. Huang, J. Liu, Q. Zhu, Catal. Today 51 (1999) 127.